The Journal of Experimental Biology 200, 1189–1200 (1997)
Printed in Great Britain © The Company of Biologists Limited 1997
JEB0568

QUANTITATIVE MODELLING OF THE EFFECTS OF SELECTED INTRACELLULAR METABOLITES ON pH IN FISH WHITE MUSCLE

PETER G. ARTHUR*, TIMOTHY G. WEST† AND PETER W. HOCHACHKA
Department of Zoology, University of British Columbia, Vancouver, British Columbia, Canada V6T 1Z4

Accepted 4 February 1997

Summary

A model is presented that provides guidelines to the identification of key experimental variables influencing proton balance and intracellular pH in vertebrate white muscle. We have drawn on data from the literature on rainbow trout (*Oncorhynchus mykiss*) in an attempt to quantify the influence of metabolic, ionic and transport components of proton generation and proton consumption after exercise. Only minor changes in proton balance and in calculated intracellular pH were caused by considering changes in the concentration of bicarbonate or including the acid–base characteristics of purine nucleotides. Intracellular pH, as estimated by the model, was more acidic at some time points in recovery compared with *in vivo* measurements, and this would appear to result mainly from inaccuracies in quantifying the phosphate component of proton buffering. Nevertheless, the model was able to simulate the typical pattern of muscle acidosis and recovery observed for trout, including the transient post-exercise acidification and the slow recovery rate. As with previous pHi models, comparison of model estimates with experimental observations is essential in this approach in order to identify whether all of the relevant metabolic processes have been considered for accurate quantification of proton balance within the white muscle compartment.

Key words: white muscle, pHi, teleosts, exercise, modelling, fish.

Introduction

Intracellular pH (pHi) is the focal measurement in studies of muscle acid–base balance. Furthermore, as a correlate and possible modulator of ion and metabolite status and as a suspected causal element of muscular fatigue, pHi regulation is likely to be crucial to the integration of homeostatic processes in active muscle. The vast experimental literature reporting on muscle acid–base equilibria indicates that pHi is predominantly a function of the proton load, the degree of intracellular buffering and the extent of proton removal from muscle. Experimentation on various animal systems has also identified many of the metabolic and ionic processes which can influence intramuscular proton balance, and these processes have been assessed quantitatively to some degree. Although our understanding of the interaction between different proton-generating and proton-consuming events is incomplete, recent experimental and theoretical analyses have begun to stress the importance of studying a more integrated view of these pathways in muscle (e.g. Pörtner 1987*a*,*b*; Schulte *et al.* 1992). Such attempts to examine the interaction between metabolic, ionic and acid–base imbalances are essential for determining which factors might have a combined influence on pHi during various acute and chronic perturbations *in vivo*.

A useful step in formulating integrated descriptions of cellular pH homeostasis is the construction of models of tissue metabolic, ionic and acid–base status. Previous theoretical treatments of proton balance and of pH regulation in animals have proved to be informative and controversial (Reeves, 1972; Stewart, 1981; Hochachka and Mommsen, 1983; Pörtner, 1987*a*,*b*; Lindinger and Heigenhauser, 1988; Tang and Boutilier, 1991) as well as motivational for experimentalists interested in manipulating pHi in these systems. In this paper, we have used primarily the studies performed on exhaustively exercised rainbow trout in an attempt to formulate a quantitative model of acidosis and recovery in white (fast-twitch, glycolytic) muscle. Fish are popular experimental animals for studying muscle metabolism because they possess large, easily accessible and relatively homogeneous white muscle masses and because they display slow, readily traceable, recoveries of levels of intramuscular metabolites. Physiological and ecological implications of species differences in burst activity and recovery rates, as well as generalizations about pHi regulation and the metabolic organization of vertebrate muscle that have been advanced from fish studies, have been

*Present address: Department of Biochemistry, University of Western Australia, Nedlands, WA 6009, Australia (e-mail: parthur@uniwa.uwa.edu.au).
†Present address: Department of Zoology, University of Cambridge, Downing Street, Cambridge CB2 3EJ, UK (e-mail: tgw1002@cus.cam.ac.uk).

discussed thoroughly elsewhere (Wood, 1991; Moyes *et al.* 1992; Arthur *et al.* 1993; Moyes and West, 1995). Our main goal with the present analysis was to use some of the more comprehensive experimental studies on the metabolism of recovery from exercise in trout (e.g. Milligan and Wood, 1986; Tang and Boutilier, 1991; Schulte *et al.* 1992) to construct an acid–base binding model for estimating the effects of varying intracellular concentrations of selected metabolites (e.g. ATP, ADP, IMP, phosphocreatine) and ions (e.g. lactate, Mg^{2+}, K^+, HPO_4^{2-}) on white muscle pHi. We gain insight into the integration of muscle pHi regulation in the sense that we can assign some quantitative significance to various processes that are known to influence, or suspected of influencing, post-exercise pHi and its recovery. Furthermore, the assumptions and short-cuts necessary for formulating a functional, if not complete, model serve to highlight some of the weaknesses in our understanding of muscle pHi regulation *in vivo*, thereby identifying areas for future experimental work.

Model equations and results

Modelling program

The model was developed on STELLA (High Perfomance Systems Inc.; Hanover, USA), which displays the different chemical relationships pictorially as the model is constructed. Any spreadsheet or mathematical program can be used to describe the model. Details of all the model equations can be supplied on request (P. G. Arthur, University of Western Australia).

Principles

Calculating changes in ion binding

The following acid–base equilibrium for phosphate is used as an example of the method used to calculate the protonation state of an intracellular buffer at a specific pH. In the reaction:

$$H_2PO_4^{1-} \rightleftharpoons H^+ + HPO_4^{2-}, \quad (1)$$

with

$$K_{eq} = [H^+][HPO_4^{2-}]/[H_2PO_4^{1-}], \quad (2)$$

where K_{eq} is the equilibrium constant, assume that phosphate was initially in the form HPO_4^{2-}. Then, in order to reach equilibrium, HPO_4^{2-} reacts with H^+:

$$([H^+] - a) + ([HPO_4^{2-}]_i - a) \rightleftharpoons ([H_2PO_4^{1-}]_i + a), \quad (3)$$

where the subscript i denotes the initial concentration and a is the amount of HPO_4^{2-} reacting with H^+. At equilibrium:

$$K_{eq} = ([H^+] - a)([HPO_4^{2-}]_i - a)/([H_2PO_4^{1-}]_i + a). \quad (4)$$

For the purposes of the model, we assumed that the pHi was temporarily constant, such that:

$$K_{eq} = [H^+]([HPO_4^{2-}]_i - a)/([H_2PO_4^{1-}]_i + a), \quad (5)$$

and after rearranging:

$$a = ([H^+][HPO_4^{2-}]_i - K_{eq}[H_2PO_4^{1-}]_i)/(K_{eq} + [H^+]). \quad (6)$$

Therefore, the final concentrations (subscript f) were:

$$[HPO_4^{2-}]_f = [HPO_4^{2-}]_i - a \quad (7)$$

and

$$[H_2PO_4^{1-}]_f = [H_2PO_4^{1-}]_i + a, \quad (8)$$

where a could be either positive or negative. The same principles describe Mg^{2+} and K^+ binding to phosphate.

Calculating pHi

By discussing a partial model, we can illustrate the principles used in the complete model. For this example, with concentrations expressed relative to the intracellular fluid compartment, we assume the following conditions: (1) initial intracelluar pH (pHi) was neutral (7.00); (2) muscle buffering capacity varied linearly with pH, and 42.5 mmol l^{-1} H^+ changed the pH from 7 to 6; (3) for simplicity, the muscle did not contain any phosphate initially; (4) the respective free concentrations of $[Mg^{2+}]$ and $[K^+]$ were 1 mmol l^{-1} and 100 mmol l^{-1}; (5) 10 mmol l^{-1} ATP was consumed to produce 10 mmol l^{-1} HPO_4^{2-} and 10 mmol l^{-1} protons.

If the only effective removal of the 10 mmol l^{-1} protons was assumed to be by intracelluar buffering (42.5 mmol l^{-1} pH $unit^{-1}$), then in the first instance ΔpH= 10/42.5=0.2353. Thus, the change in pHi was initially calculated as pHi=7.0000–0.2353=6.7647. The 10 mmol l^{-1} HPO_4^{2-} generated will bind H^+, Mg^{2+} and K^+. The following K_{eq} values were used for these reactions:

$$H_2PO_4^{1-} \rightleftharpoons H^+ + HPO_4^{2-} \quad K_{eq}' = 1.996\times10^{-7}, \quad (9)$$

$$MgHPO_4 \rightleftharpoons Mg^{2+} + HPO_4^{2-} \quad K_{eq}' = 3.239\times10^{-2}, \quad (10)$$

$$KHPO_4^{1-} \rightleftharpoons K^+ + HPO_4^{2-} \quad K_{eq}' = 3.386\times10^{-1}. \quad (11)$$

These values were derived from standard values of K_{eq}' using the temperature and ionic strength adjustment shown in the Appendix. In subsequent model iterations, the expected equilibrium concentrations of $H_2PO_4^{1-}$, $MgHPO_4$ and $KHPO_4^{1-}$ were estimated assuming that $[HPO_4^{2-}]$= 10 mmol l^{-1}, that pHi=6.7647 and that $[Mg^{2+}]$ and $[K^+]$ remained at 1 mmol l^{-1} and 100 mmol l^{-1}, respectively.

The iterative process for estimating pHi and the equilibrium concentrations of the various forms of phosphate, i.e. bound to H^+, Mg^{2+} and K^+, was repeated until the changes in the concentration of each of the compounds was less than approximately 0.5 %. An example of the results from this method is shown in Table 1. Note that two data sets are presented for each variable estimated, using a (as defined in equation 3) and 0.6a. The fractional solutions to the equations (using 0.6a) allowed the model to converge to the appropriate tolerance limit with fewer iterations and with less instability, particularly with the complete model where many more binding equations had to be considered simultaneously. The complete model contained 26 binding equations and required 40 iterations to achieve the desired level of accuracy.

Table 1. *Example of the results from the iterative method used to estimate pHi*

		Iteration						
		1	2	3	4	5	10	20
[Total phosphate]		10	10	10	10	10	10	10
$[HPO_4^{2-}]$	*x*	0	5.0533	4.6736	4.6296	4.6191	4.6100	4.6098
	y	0	1.7555	6.1050	3.8134	5.0285	4.6190	4.6098
$[H_2PO_4^{1-}]$	*x*	0	2.7764	3.1000	3.2111	3.2596	3.3163	3.3171
	y	0	4.6273	2.5614	3.7132	3.1104	3.3126	3.3171
$[MgHPO_4]$	*x*	0	0.8024	7.9077	0.7547	0.7339	0.7120	0.7116
	y	0	1.3373	4.1358	0.8717	0.6265	0.7098	0.7116
$[KHPO_4^{1-}]$	*x*	0	1.3680	1.4256	1.4046	1.3873	1.3624	1.3614
	y	0	2.2800	0.9200	1.6017	1.2346	1.3587	1.3614
Protons produced		10	10	10	10	10	10	10
Protons consumed	*x*	0	2.7764	3.1100	3.2110	3.2696	3.3155	3.3171
	y	0	4.6273	2.5614	3.7131	3.1104	3.3126	3.3171
ΔpH	*x*	−0.2353	−0.1700	−0.16211	−0.1597	−0.1586	−0.1573	−0.1572
	y	−0.2353	−0.1264	−0.1750	−0.1479	−0.1621	−0.1574	−0.1572
pHi	*x*	6.7647	6.8300	6.8379	6.8403	6.8414	6.8427	6.8428
	y	6.7647	6.8736	6.8250	6.8521	6.8379	6.8426	6.8428

Total phosphate was assumed to be 10 mmol l^{-1}. *x* is a factor of 0.6, *y* is a factor of 1 for a as in equation 3.

Complete model

Relationships between components

The model itself is composed of several parts. Simplified examples of the equations are described below without most the conditionals included in the computer model. These kinds of equations are described for a system where the initial concentrations (subscript i) of phosphocreatine (PCr), ATP, ADP, AMP, IMP, inosine, ammonia, lactate and pH, as well as the final concentrations (subscript f) of PCr, ATP, ADP, AMP, IMP and lactate, were defined. For each enzyme or system specified, each of the primary components is identified and is separated by '&'. To avoid confusion, we use '&' instead of '+' to indicate participation in a reaction that is not explicitly included in the arithmetic equation. At every iteration, each equation is solved fractionally by using a value of *a* between 0 and 1, generally 0.6 as described above. As examples, the components of the creatine kinase equilibrium and of ATPase activity were formulated as follows.

For creatine kinase:

$$(H^+\ load_{total(x)} - a)\ \&\ (ADP_{total(x)} - a)\ \&\ (PCr_{total(x)} - a) \rightleftharpoons (Cr_{total(x)} + a)\ \&\ (ATP_{total(x)} + a), \quad (12)$$

where $a=(PCr_{total(i)}-PCr_{total(f)})0.6$.

For ATPases:

$$(ATP_{total(x)} - b) \rightleftharpoons (ADP_{total(x)} + b)\ \&\ (P_{i,total(i)} + b)\ \&\ (H^+\ load_{total(x)} + b), \quad (13)$$

where $b=(ATP_{total(i)}-ATP_{total(f)})0.6$.

In equation 13, *b* has the same meaning as *a*, as defined in the previous section. Similar equations described the adenylate kinase, AMP deaminase and 5′-nucleotidase equilibria and glycolysis (i.e. lactate formation). Initial calculations were based on pre-exercise concentrations measured in the tissue. For each metabolite, the subscript 'total' refers to the combined concentrations of all metabolites, including bound and ionic forms, such that: $[Metabolite]_{total} = \sum[Metabolite]_{free} + \sum[Metabolite]_{bound}$ = measured concentration, adjusted to intracellular volume. For the examples above, the effect of changes on the main model after each iteration (denoted by subscript 'x') were $\Delta[PCr]_{total(x)}=-a$, $\Delta[Cr]_{total(x)}=a$ and $\Delta[ATP]_{total(x)}=a-b-c$ for ATP, where *c* in this example is the change in [ATP] resulting from the adenylate kinase component of the model. Changes in ADP, AMP, IMP, inosine, phosphate and ammonia concentrations and proton load were accounted for in the same manner.

This part of the model described the stoichiometric relationships between the various substrates and products, but did not give any information about ionic composition. For example, this part of the model was used to indicate that hydrolysis of one ATP molecule produced one ADP molecule, one proton and one HPO_4^{2-} molecule. Inclusion of ionic binding calculations, described in the following section, indicates that hydrolysis of one ATP molecule actually produces only a fraction of a proton.

It is important to emphasize that these calculations are merely a method of counting the various components of the system. Although the chemical reactions are catalysed by enzymes *in vivo*, no information about the kinetics of the

various enzymes involved was required. In a kinetic model, the correct substrates would be required (e.g. $MgATP^{2-}$) along with the kinetic parameters for each enzyme (K_m, V_{max}, etc.). Enzyme names were used in the model as a reminder that some reactions were enzymatic reactions as opposed to acid–base dissociation or magnesium binding equilibrium reactions.

Ionic sub-models

Many intramuscular metabolites can participate in ion-binding reactions *in vivo*. These processes are described as a series of ionic sub-models calculated for ATP, ADP, AMP, IMP, phosphate, bicarbonate and PCr. The binding of these compounds to H^+, Mg^{2+} and K^+ was described for those cases where binding constants were available. As an example, we describe the ionic sub-model for AMP. First, $[AMP]_{total(x)}$ from the main model was matched to the sum of the ionic components. Note that changes in $[AMP]_{total(x)}$ caused AMP to leave or enter the ion binding model as AMP^{2-}. Thus, we have assumed that all reactions involve only the anionic form of each compound. Clearly, this does not happen *in vivo* but, as this is not a kinetic model, it was not necessary to describe in more detail the nature of the compounds participating in the reactions.

The connection with the main model was:

$$\begin{aligned}[AMP]^{2-}_{(x)} &= [AMP^{2-}]_{(x-1)} + 0.6\Delta[AMP]_{total(x)} \\ &= [AMP^{2-}]_{(x-1)} + 0.6([AMP]_{total(x)} - \Sigma[AMP]_{ionic(x-1)}) \\ &= [AMP^{2-}]_{(x-1)} + 0.6\{[AMP]_{total(x)} - ([AMP^{2-}]_{(x-1)} \\ &\quad + [HAMP^{1-}]_{(x-1)} + [H_2AMP]_{(x-1)} + [MgAMP]_{(x-1)} \\ &\quad + [KAMP^{1-}]_{(x-1)})\}. \qquad (14)\end{aligned}$$

Binding in the ionic sub-model was described by four equations that account for [MgAMP], [HAMP], $[H_2AMP]$ and [KAMP]. For example, the equation for Mg^{2+} binding appeared as:

$$([MgAMP]_{(x-1)} - d) \rightleftharpoons ([AMP^{2-}]_{(x)} + d) \;\&\; ([Mg^{2+}] + d), \qquad (15)$$

where

$$d = \{(K_{eq,MgAMP}[MgAMP]_{(x-1)} - [AMP^{2-}]_{(x)}[Mg^{2+}])/([Mg^{2+}] + K_{eq,MgAMP})\}0.6. \qquad (16)$$

At each iteration in the ionic sub-model, $\Delta[AMP^{2-}]_{(x)}$, $\Delta[HAMP^{1-}]_{(x)}$, $\Delta[H_2AMP]_{(x)}$, $\Delta[MgAMP]_{(x)}$, $\Delta[KAMP^{1-}]_{(x)}$, ΔProton $load_{(x)}$, $\Delta[Mg^{2+}]_{(x)}$ and $\Delta[K^+]_{(x)}$ could be determined in the same manner as described for components in the main model (using K_{eq}' values calculated from data in the Appendix).

To calculate the change in pHi, we used an amino buffering capacity of 42.5 mol H^+ per pH unit per millilitre of intracellular water, as estimated by Abe *et al.* (1985). This buffering capacity was termed 'amino buffering' to indicate that it did not include a phosphate buffering component as is typically measured in homogenates (Milligan and Wood, 1986). The intracellular pH could then be calculated from the change in proton loading and buffering capacity. The new pHi after each iteration would be:

$$pHi_{(x)} = pHi_{ref} + \Delta pHi_{(x)} = pHi_{ref} + (\text{proton load}_{(x)}/\text{buffering capacity}), \qquad (17)$$

where pHi_{ref}, the reference pHi, was normally the pHi of muscle measured in resting fish. In addition, it was also possible, with a slight modification of the model, to estimate generated and consumed proton loads at a defined pHi.

Assumptions and experimental data

Where possible, we have used experimental data in the model, and because of the completeness of their data set we gave preference to the work of Schulte (1990) and Schulte *et al.* (1992). The main assumptions made in applying data were as follows.

(1) Metabolite concentrations were adjusted from $\mu mol\,g^{-1}$ to $mmol\,l^{-1}$ assuming a constant fluid volume of $0.72\,ml\,g^{-1}$ wet tissue mass (Schulte *et al.* 1992).

(2) Total creatine (Cr+PCr) concentration in muscle was assumed to be constant ($58\,mmol\,l^{-1}$).

(3) Only free phosphate participated in acid–base reactions. Based on nuclear magnetic resonance (NMR) estimates of [PCr], $1\,mmol\,l^{-1}$ free phosphate was assumed and 84 % of total creatine appeared as PCr (van Waarde *et al.* 1990). Changes in free phosphate concentration were based on these pre-exercise estimates and it was assumed that post-exercise phosphate was derived from PCr, ATP, ADP and AMP.

(4) All of the ADP was assumed to be available to participate in ion- and proton-binding reactions.

(5) Pre-exercise $[NH_4^+]$ was assumed to be $0.9\,mmol\,l^{-1}$ (estimated from Tang *et al.* 1992). Post-exercise changes were assumed to be generated from AMP degradation to IMP and NH_4^+ *via* AMP deaminase. Model estimates of post-exercise $[NH_4^+]$ ($8.2\,mmol\,l^{-1}$) were comparable to measurements by Tang *et al.* (1992) of $9.4\,mmol\,l^{-1}$.

(6) The influence of changes in P_{CO_2} on pHi (as modelled previously by Pörtner, 1987*b*) was based on a resting P_{CO_2} of 0.3 kPa (2.25 mmHg) and a post-exercise $P_{CO_2\ of}$ 1.2 kPa (9 mmHg) (Tang *et al.* 1992).

(7) Post-exercise IMP appearance was attributed exclusively to adenylate hydrolysis. Purine nucleotides were conserved in the model, and [IMP] during recovery was the difference between the total purine nucleotide pool and the summed concentrations of ATP, ADP and AMP. Post-exercise [IMP] was estimated at $7.67\,mmol\,l^{-1}$ in the model, whereas Schulte *et al.* (1992) measured $7.33\,mmol\,l^{-1}$.

(8) Model reactions are shown as being directly reversible, which of course does not occur *in vivo*. As an example, post-exercise resynthesis of AMP occurs *via* an intermediate metabolite, adenylosuccinate, rather than directly from IMP (Mommsen and Hochachka, 1988). An explicit model of AMP formation would include pre-exercise concentrations of adenylosuccinate, aspartate, GTP, GDP and fumarate.

However, with respect to protons, ammonia and phosphate, and since it is known that the sum of ATP, ADP, AMP and IMP concentrations remains essentially stable during exercise and recovery, the resynthesis of AMP could be summarized as the reversal of AMP deaminase in the present model.

(9) The small amount of lactate exported from white muscle after exercise was assumed to be associated with the removal of protons in a 1:1 stoichiometry (Poole and Halestrap, 1993). We have accounted for the small amount of H^+ that appears in plasma in excess of lactate immediately post-exercise (amounting to an approximate reduction of 0.143 mmol l^{-1} in the muscle, following Tang *et al.* 1989, and assuming blood volume and muscle mass were respectively 3 % and 60 % of body mass), but we have not modelled specifically any proton losses from muscle that might occur independently of lactate movements throughout recovery (e.g. by specific ion-exchange mechanisms).

Results and discussion

Comparison with existing formats

Changes in proton concentrations as a result of PCr or ATP hydrolysis are described typically in a fractional form (Hochachka and Mommsen, 1983; Pörtner, 1987*a*). The results of this model can also be written in this format. As an example, consider ATP hydrolysis ($ATP^{4-} \rightleftharpoons ADP^{3-}+H^+ +HPO_4^{2-}$). Changes in the concentration of each of the components cause fractional displacements in the various binding reactions, and the degree of change will correspond to the fraction in that form. If [ATP^{4-}] is 11.8 % of total [ATP], then the fractional change will be 0.118[ATP^{4-}] (as is shown in Table 2).

The proton load: where does it come from and where does it go?

To assess the importance of various metabolites in affecting the pHi of trout white muscle, we have partially described the intramuscular environment before and after exhaustive exercise (Table 3). The estimated pHi was a relatively good match to measured pHi values, and it was apparent that only a few critical measurements were required in order to predict muscle pHi.

Substantial amounts of H^+ were generated as the result of enzyme-catalysed reactions. Quantitatively, the oxidation of glycogen to lactate, producing 51 mmol l^{-1} H^+, and the hydrolysis of adenylates to IMP, adding another 14.5 mmol l^{-1} H^+, were the main reactions contributing to the total proton load (Table 3). Ultimately, deamination of AMP to IMP helped to reduce the muscle proton load since approximately half of the H^+ generated initially by ATP and ADP hydrolysis became bound to NH_3. Regeneration of ATP from PCr breakdown did not, in itself, change the overall proton load since H^+ utilized in the creatine phosphokinase reaction (30 mmol l^{-1}) was

Table 2. *Ionic composition before and after exercise as a percentage of the total concentrations described in Table 3*

		X	H*X*	H_2X	Mg*X*	Mg_2X	MgH*X*	K*X*
Bicarbonate	Pre	92.10	7.90					
	Post	70.80	29.20					
Ammonia	Pre	0.30	99.70					
	Post	0.06	99.94					
Phosphocreatine	Pre	98.30	0.20		1.50			
	Post	97.60	0.90		1.50			
ATP	Pre	11.80	1.93	0.001	66.86	2.03	0.126	17.20
	Post	10.91	8.51	0.024	62.29	1.90	0.550	15.80
ADP	Pre	40.20	4.81	0.003	26.10		0.091	28.78
	Post	33.90	19.38	0.052	22.00		0.367	24.22
AMP	Pre	63.75	5.14	0.002	2.41			28.70
	Post	53.36	20.56	0.045	2.02			24.02
IMP	Pre	65.60	4.44	0.002	0.51			29.50
	Post	56.10	18.20	0.040	0.43			25.20
Phosphate	Pre	57.30	17.30		1.80			23.70
	Post	34.60	50.00		1.10			14.30

At pHi 7.22, 1 mmol l^{-1} Mg^{2+} and 140 mmol l^{-1} K^+, the overall fractional forms for ATP and ADP prior to exercise will be: $0.118ATP^{4-}+0.669MgATP^{2-}+0.020Mg_2ATP+0.019HATP^{3-}+0.00001H_2ATP^{2-}+0.00126MgHATP^{1-}+0.172KATP^{3-}+0.353K^+ \rightleftharpoons 0.402ADP^{3-}+0.261MgADP^{1-}+0.0481HADP^{2-}+0.00003H_2ADP^{1-}+0.00091MgHADP+0.2878KATP^{2-}+0.573HPO_4^{2-}+0.173H_2PO_4^{1-}+0.018MgHPO_4+0.237KHPO_4^{1-}+0.430Mg^{2+}+0.798H^+$.

In this example, the amount of Mg^{2+} produced was determined by adding the fractional substrates containing Mg^{2+} and subtracting the fractional products containing Mg^{2+}. The amounts of K^+ consumed and H^+ produced could also be determined in a similar manner.

X is the percentage of each metabolite or ion calculated in its free, or H^+-, Mg^{2+}- and K^+-bound forms.

Table 3. *The effect of exercise on pHi in the white muscle of trout as estimated by the model and as measured by the homogenate and the DMO methods*

	Pre-exercise	Post-exercise	Protons produced		Protons consumed	
			(mmol l^{-1})	(%)	(mmol l^{-1})	(%)
pHi (modelled)		6.54				
pHi (DMO)	7.22	6.78±0.11				
pHi (homogenate)	7.27	6.64±0.03				
[Lactate] (mmol l^{-1})	6.74	57.94	51.20	77.90		
Amino buffering (μmol pH $unit^{-1}$)	42.50	42.50			28.31	43.10
Total CO_2 (mmol l^{-1})	2.51	2.45			0.69	0.01
Total [NH_3] (mmol l^{-1})	0.92	8.22*			7.30	11.10
[PCr] (mmol l^{-1})	36.43	5.92	0.02	0.02		
[Total phosphate] (mmol l^{-1})	14.12†	59.15*			27.76	42.30
[Total ATP] (mmol l^{-1})	9.75	2.53			0.02	0.04
[Total ADP] (mmol l^{-1})	0.98	0.91			0.14	0.20
[Total AMP] (mmol l^{-1})	0.07	0.09			0.02	0.02
[Total IMP] (mmol l^{-1})	0.39	7.67*			1.46	2.21
Hydrolysis of adenylates to IMP			14.54	22.10		
Creatine kinase reaction					30.50	NA
Hydrolysis of ATP formed from PCr			30.50	NA		
Total H^+ load (mmol l^{-1})			65.76			

Data for *Oncorhynchus mykiss* are taken from Schulte *et al.* (1992).

The processes by which protons were produced and consumed are also shown.

*As explained in the text, the experimental results have been replaced by results generated by the model.

†We assumed that the concentration of phosphate in the resting fish was 1 mmol l^{-1} and that, when measured, the breakdown of phosphocreatine (PCr) liberated another 13.122 mmol l^{-1} phosphate.

Post-exercise pHi values are means ± S.E.M. (*N*=7).

DMO, 5,5′-dimethyl oxazolidine-2,4′-dione.

NA, not applicable.

liberated by subsequent ATP hydrolysis during the period of net decline in cellular ATP concentration.

One of the principal buffers of a post-exercise proton load is intracellular phosphate derived from the breakdown of PCr and ATP. Inorganic phosphate (P_i) is liberated as the end-products of ATP and PCr hydrolysis (IMP and creatine) accumulate; immediately after exercise, approximately 68 % of the muscle P_i is expected to have been derived from PCr. Phosphate from these sources buffered approximately 42 % of the total proton load in exercised muscle over the pH range 7.3–6.6 (Table 3). Phosphate derived from hydrolysis of ATP to IMP, together with the buffering effect of NH_3, consumed not only all of the protons produced during these reactions (i.e. reactions converting ATP to IMP), but also an extra 2 mmol l^{-1} of protons. The importance of phosphate buffering can also be demonstrated by considering the relationship between post-exercise acidosis and non-steady-state energetics. On the basis of cellular losses of ATP, PCr and glycogen, approximately 84 mmol l^{-1} equivalents of ATP are turned over during burst exercise, with a net production of 28 mmol l^{-1} of protons which need to be buffered. By comparison, if the 84 mmol l^{-1} equivalents of ATP were generated solely by glycogenolysis, then 56 mmol l^{-1} of protons would be produced. Overall, the enzymatic breakdown and loss of cellular PCr and ATP resulted in net consumption of protons. Exercise-induced elevation of phosphate concentration is obviously useful for buffering metabolic protons, although this benefit may be partially negated in physiological systems since a build-up of diprotonated phosphate is one possible mechanism of muscle fatigue (Westerblad *et al.* 1991).

Adenylates also had the potential to influence the proton load. In the resting fish, the adenylate pool appeared primarily as MgATP. There was very little protonated ATP (Table 2). In contrast, there was a substantial amount of IMP after exercise and, since its binding to Mg^{2+} was weak, a large fraction of the IMP was protonated. As a result, there was a net binding of H^+ by adenylates after exercise in comparison with muscle in the pre-exercise state (Table 3). Nevertheless, the impact on total proton load was minor, with less than 3 % of the proton load being removed by acid–base reactions with the adenylates.

Bicarbonate buffering can affect H^+ load in the sense that CO_2 formation effectively transfers equivalents to the extracellular environment. However, total bicarbonate concentration is low in fish white muscle, and it is not likely that even rapid removal of bicarbonate-buffered H^+ immediately after exercise would contribute significantly to total proton buffering by other intracellular buffers. The impact of HCO_3^- on the metabolic acid load was small (Table 3).

The other important buffers, collectively described as

Table 4. *Effects of some variables on model estimates of pHi before and after exhaustive exercise*

	Pre-exercise	Exhaustion	Recovery time (h) 2	4	8	24
Reference estimates[1]	7.266	6.549	6.460	6.551	6.830	7.216
Change reference pHi to 7.400[2]	7.442	6.661	6.609	6.696	6.987	7.396
Reduce ionic strength by 10 %[3]	7.227	6.553	6.462	6.553	6.832	7.216
Temperature 25 °C[3]	7.255	6.546	6.509	6.595	6.866	7.215
P_{CO_2} = 0 kPa[4]	7.271	6.544	6.436	6.529	6.812	7.215
Reduce post-exercise [K^+] from 140 to 120 mmol l^{-1} [5]	7.267	6.556	6.464	6.555	6.834	7.216
[K^+] and [Mg^{2+}] = 0 mmol l^{-1} [6]	7.268	6.606	6.502	6.596	6.859	7.216
[Mg^{2+}] = 6 mmol l^{-1} [7]	7.266	6.532	6.446	6.537	6.812	7.216
Free [phosphate] = 10 mmol l^{-1} [8]	7.263	6.597	6.532	6.612	6.864	7.216
Halve K_{eq} for free phosphate (i.e. change pK from 6.7 to 7.0)[9]	7.272	6.650	6.505	6.607	6.878	7.216
Assume total creatine is 85 % phosphorylated[10]						
Reference pHi = 7.22	7.307	6.572	6.490	6.581	6.864	7.257
Reference pHi = 7.40	7.470	6.677	6.629	6.717	7.011	7.425

(1) Initial estimates assumed a reference pHi of 7.22 (homogentate technique; Schulte *et al.* 1992), [phosphate] = 1 mmol l^{-1}, temperature = 15 °C, [Mg^{2+}] = 1 mmol l^{-1}, [K^+] = 140 mmol l^{-1} and [PCr] = 26.2 mmol l^{-1}, which is 62 % of [total Cr].

(2) Reference pHi of 7.4 comes from NMR studies (van den Thillart *et al.* 1989).

(3) Changes in ionic strength and temperature had a minor effect on pHi. Note, however, that amino buffering, a major proton consumer, could not be described as a function of either variable.

(4) Assuming that intramuscular P_{CO_2} is zero had little effect on pHi.

(5) Extra K^+ (<5 mmol l^{-1}) was assumed to become bound, mainly to phosphate, after exercise. The effect was to increase H^+ load as the amount of phosphate and IMP that could bind protons was reduced. [K^+] is typically reduced in animals after exercise, but even if [K^+] was modelled to exceed the decline seen in rats (approximately 15 mmol l^{-1}; Lindinger and Heigenhauser, 1988), the effect on pHi was negligible.

(6) Conversely, increased buffering of protons (from phosphate and adenylates) occurred when concentrations of the metal ions [K^+] and [Mg^{2+}] were set at 0 mmol l^{-1} in the model. The effect of changing [Ca^{2+}] was not modelled.

(7) Free [Mg^{2+}] ranges from 0.5 to 5 mmol l^{-1} (Brinley *et al.* 1977; Curtin and Woledge, 1978; Borchgrevink *et al.* 1989; Murphy *et al.* 1989). 1 mmol l^{-1} was assumed in the general model. Even if [Mg^{2+}] was increased by 5 mmol l^{-1}, from Mg^{2+} released from adenylates, the effect on pHi was minor.

(8) Estimates of [phosphate] made by chemical means and by NMR can be as high as 10 mmol l^{-1}, even when allowing for PCr hydrolysis during sampling for chemical analysis (Schulte, 1990). This phosphate may be unavailable to buffer changes in pHi if it is in a different cellular compartment or if it is bound to intracellular proteins. Increasing [phosphate], to values ten times higher than NMR estimates of 0.5–1 mmol l^{-1} (van Waarde *et al.* 1990), changes the model estimate of post-exercise pHi by 0.05 units.

(9) Error in phosphate affinity for H^+ in the model had a substantial impact on the estimate of pHi at exhaustion. Phosphate binds 42 % of an H^+ load using pK=6.7 (Alberty and Goldberg, 1992), whereas a higher pK value of 7.0 (Phillips *et al.* 1965; Curtin and Woledge, 1978) increases H^+ binding to almost 50 %.

(10) NMR studies indicate that 85 %, or more, of the total creatine pool is phosphorylated (van Waarde *et al.* 1990). The impact of assuming a value of 85 % was that all estimates of pHi were slightly alkaline relative to estimates made when creatine phosphorylation state was assumed to be lower (62 %; Schulte *et al.* 1992).

'amino buffering', consumed almost 43 % of the protons (Table 3). Amino buffering is a relatively crude measurement describing the combined buffering capacity of proteins, amino acids and soluble histidine compounds in white muscle (Abe *et al.* 1985). It is obviously important to have an accurate description of the buffering capacity of these compounds. The estimate of Abe *et al.* (1985) appears to be the only measurement of non-phosphate buffering capacity in trout white muscle. Nevertheless, this estimate appeared to be reasonable given that total buffering capacity, which included the phosphate component, was 56.7 μmol NaOH pH $unit^{-1}$ g^{-1} and was comparable to the estimate of 51.32 μmol H^+ pH $unit^{-1}$ g^{-1} obtained by Milligan and Wood (1986).

Variation in model estimates of pHi

Table 4 lists some variables for which values were assigned primarily on the basis of variability in literature values that result mainly from differences in measurement technique. The model appears to be fairly robust in the sense that alterations in these variables generally produced only moderate deviations (of up to 0.1 pH unit) from results calculated in the original reference model (see Table 4).

Changes in some of the inorganic ion concentrations

affected the model. However, the combined effect of K^+ and Mg^{2+} was evident only when these ions were excluded from the model (Table 4). Changes in concentrations of K^+ and Mg^{2+} that might be expected following strenuous exercise had essentially no effect on pHi (Table 4). In the case of phosphate ions, the model was run using concentrations determined either chemically or by NMR. NMR measurements are expected to describe unbound phosphate levels and are usually lower than total phosphate concentrations measured by enzymatic means. While it is clear that phosphate is an important buffer in the system, there would be, nevertheless, only slightly more H^+ bound to phosphate after exercise if it was assumed that total (enzymatically measured) cellular phosphate was available to buffer changes in pHi. A 10-fold difference in muscle phosphate concentration before exercise caused a shift in pHi of 0.05 unit immediately after exercise (Table 4). In addition, the transient acidification evident at 2–4 h of the recovery period was damped when the model was run with the extra phosphate available.

A potentially serious problem was the quantification of proton affinity with each of the ion components. Given the overall importance of phosphate in buffering protons, a physiologically relevant description of phosphate affinity for H^+ was essential for accurate comparison of *in vivo* pHi changes with model estimates of pHi. As is shown in Table 4, the effect of altering the pK (from 6.7 to 7.0, equivalent to halving K_{eq}) for proton–phosphate affinity was to increase the estimate of pHi by 0.1 unit at the time of exhaustion. On the basis of homogenate studies, the reaction pK should be close to 6.8 (Pörtner, 1990). Our only point here is that substantial error in the value of K_{eq} for this ion dissociation reaction in particular has the potential to alter significantly the outcome of the model. Other ion–proton interactions used in the model were less important than the phosphate–proton affinity and had little effect on pHi.

As with measurements of cellular phosphate concentration, NMR and chemical measurements of pHi tend to vary (Table 4). Choice of a 'reference' pHi clearly could affect the model estimates, given that this value serves as a reference for subsequent calculations of pHi. The effect of assuming a more alkaline reference pHi (7.4; based on NMR) was to increase pHi prior to exercise, as well as at exhaustion and throughout recovery. Nevertheless, the pattern of recovery from acidosis was similar regardless of the reference pH used to run the model.

Comparisons with in vivo *observations*

We used existing data (from Schulte *et al.* 1992) on rainbow trout white muscle metabolism in order to make gross comparisons and contrasts of model estimates of pHi recovery with a typical *in vivo* recovery pattern (Fig. 1). Model estimates of muscle pHi using different starting concentrations of PCr and phosphate were also included for comparison (Fig. 1; Table 4). The basic model was a good approximation of changes in pHi throughout recovery, with the notable anomaly that pHi immediately (time 0 h) after exercise and at 8 h into recovery underestimated *in vivo* results, particularly those obtained using the DMO method (experimental data obtained using the homogenate technique, a method of direct measurement of pHi in metabolically inhibited muscle homogenates, Pörtner *et al.* 1990, were less variable and were lower than mean estimates of pHi measured using the DMO technique). The overall effect of changing phosphate concentration was to bring the model estimates into closer agreement with the *in vivo* measurements of pHi and, as was noted earlier, to dampen the post-exercise acidification that appeared to be somewhat exaggerated in the reference model.

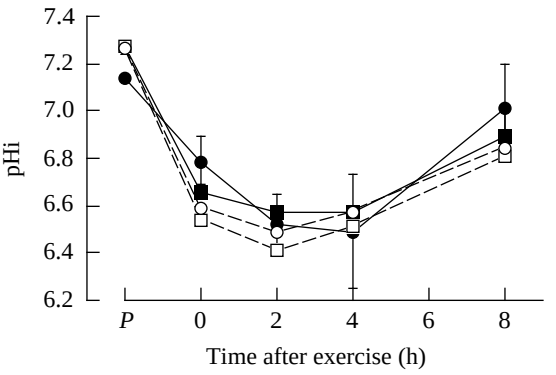

Fig. 1. The relationship between model results and experimental results during recovery from exercise. The experimental measurements of pHi in rainbow trout muscle by the homogenate technique (filled squares) and the DMO technique (filled circles) of Schulte *et al.* (1992) are shown. Standard error bars are shown (N=7). Two scenerios are presented: (1) in the resting fish, phosphocreatine concentration is as measured experimentally, but [phosphate] was 14 mmol l^{-1} (open circles); and (2) all metabolite concentrations are as measured experimentally (open squares). *P*, pre-exercise value.

We cannot confirm the physiological relevance of altering any particular component in the model in order to bring the results into line with experimental observations. On the one hand, the effect of changing phosphate concentration (Fig. 1) suggests that phosphate availability and PCr phosphorylation state must be defined appropriately. On the other hand, underestimation of pHi may mean that 'amino buffering' capacity was underestimated or that there are other buffers that should have been included in the model. The latter possibility would appear to be unlikely, given that the gross measure of buffering capacity of muscle should include not only known buffers but also unknown buffers. It is also possible that we have not accurately estimated the buffering capacity of one or more components described in the model. For example, as was discussed previously, it is critical to be accurate with estimates of the association constant for proton binding by phosphate. Finally, the amino buffering capacity of the muscle is measured in terms of μmol of H^+ (or OH^-) required to change the pH by 1 unit. This assumes a linear relationship between pH and the quantity of acid, or base, added. Although crude homogenates containing phosphate do show this relationship, it should be experimentally verified that the combined amino buffers show a similar relationship.

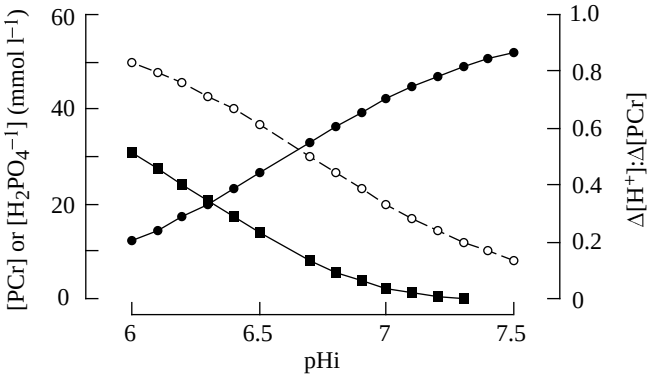

Fig. 2. The contribution of phosphocreatine to buffering within the cell as determined in the model, assuming that 85 % of all creatine in the cell is phosphorylated at pH 7.3 and that the concentration of ATP does not change. The concentration of phosphocreatine (PCr, filled circles) and the concentration of protons bound as $H_2PO_4^{1-}$ (filled squares) are shown (left-hand axis) as changes in pHi cause a shift in the creatine kinase equilibrium. The model indicates that the ratio of the change in $[H^+]$ to the change in [phosphocreatine] (right-hand axis) decreases, from above 0.8 at pHi 6 to just below 0.2 at pHi 7.5 (open circles).

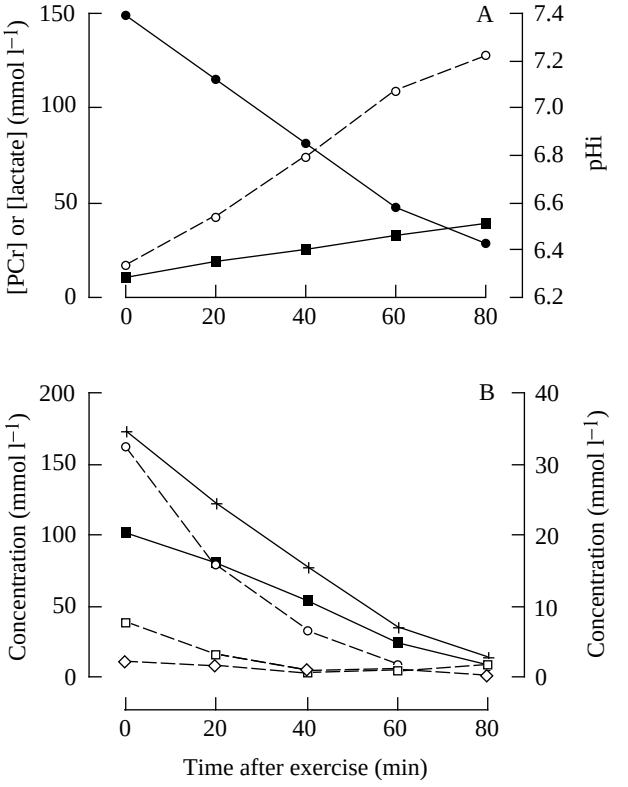

Fig. 3. (A) Recovery from exercise in a tuna, *Katsuwonus pelamis*, muscle showing predicted pHi (open circles) with changes in phosphocreatine (filled squares) and lactate (filled circles) concentration, as measured by Arthur *et al.* (1992). (B) The generated proton load (crosses, left axis) is consumed by amino buffering (filled squares, left axis), phosphate (open circles, right axis), ammonia (open squares, right axis) and other compounds (open diamonds, right axis) such as adenylates. The figure indicates $[H^+]$ generated which the model predicts to be bound by each of the major buffers identified.

The characteristics that most resembled experimental observations were the transient post-exercise acidification and the slow overall recovery of pHi. Short-term acidification in muscle has been observed in a number of studies of exercise (Milligan and Wood, 1986; Tang and Boutilier, 1991; Schulte *et al.* 1992) and during recovering from anoxia (van Waarde *et al.* 1990) in fish. Analysis of the model provides an interpretation that involves two opposing processes, as described previously (van Waarde *et al.* 1990). During the initial phase of recovery, there was a rapid increase in the concentration of PCr, which was dictated largely by the sensitivity of the creatine kinase equilibrium to H^+ concentration and changes in the $[ATP]_{free}/[ADP]_{free}$ ratio. It would seem that the early rise in PCr concentration resulted mainly from a precipitous decline in the concentration of $[ADP]_{free}$. Formation of PCr in this manner alone is expected to produce H^+ but, there is no net change in H^+ balance during the synthesis of PCr in the face of a constant [ATP]. However, H^+ production occurred independently, via the release of protons from phosphate incorporation into ADP. In turn, the amount of H^+ produced depended on the fraction of phosphate in the diprotonated form (Fig. 2). Thus, resynthesis of PCr produced more protons at pH 6.5 (approximately 0.6 proton per PCr molecule), when diprotonated phosphate concentration was highest, than at pH 7.3 (approximately 0.2 proton per PCr molecule). Post-exercise acidification persisted for at least 2 h, a relatively short period given the overall pace of the recovery process (requiring up to 24 h). The acidification is viewed as transient since it is the overall recovery that counterbalances the decline in pHi by removing protons from the system; i.e. *via* resynthesis of ATP from IMP, by glyconeogenesis, by lactate oxidation and by proton losses to the extracellular compartment, possibly *via* cotransport with lactate (Juel and Wibrand, 1989; Mason and Thomas, 1988; Schulte *et al.* 1992; Moyes and West, 1995).

An interesting feature of the model was that the relative importance of phosphate as a buffer became progressively reduced throughout recovery: phosphate bound 42 % of the H^+ load immediately after exercise, 37 % at 2 h post-exercise, and just 26 % after 8 h (calculations not shown). This was a function both of reduced binding of H^+ to phosphate as the pH became more alkaline and of the reduced phosphate concentration as ATP and PCr were resynthesized. We are not aware of experimental observations that address these calculations directly, and so it would be of interest in a future study of the metabolism of fish during recovery from exercise to focus specifically on the role of phosphate dynamics in post-exercise acid–base balance.

The aim of this exercise was to describe the main components of proton balance, including enzymatically catalysed reactions and those involved in acid–base reactions, in the trout white muscle system so as to provide an integrative and quantitative model of the effects of exercise and recovery on pHi. A model based on a few key variables produced pHi

estimates that were in general accord with existing empirical observations of trout muscle acidosis and recovery. Although pHi values from the basic 'reference' model were more acidic than experimental observations at two points in the recovery period, the overall *in vivo* pattern of recovery was reproduced quite well. The weaknesses in the model (e.g. imprecision regarding the amount of enzymatically measured phosphate contributing to the overall buffering) identify gaps in our knowledge of quantitative proton buffering and fluxes, and the heuristic value of such modelling exercises to future investigation is that they draw attention to areas which might otherwise be overlooked in experimental designs. In general, the capacity to simulate changes in pHi suggests that the model presented is a reasonable reflection of the influence of the intracellular environment on proton metabolism, emphasizing that H^+ concentration is, in essence, mainly dependent on a few key metabolites of anaerobiosis.

Ultimately, it would be of interest to adapt a model to different muscle systems (e.g. across species and different muscle types) that display different performance characteristics and rates of recovery. One system that we have explored superficially with the model is the white muscle of skipjack tuna *Katsuwonus pelamis*, which has comparatively high glycolytic and oxidative capacities and is known to recover rapidly (<2 h) from burst exercise. We are able to provide some interpretation of metabolic events that have not

Appendix

K_{eq} and ΔH° values for the ionic dissociation reactions at zero ionic strength and 25 °C

	Reaction	K_{eq}	$\Delta H°$	Reference
Bicarbonate	$H_2CO_3 \rightleftharpoons HCO_3^{1-}+H^+$	4.352×10^{-7}	7660	Curtin and Woledge (1978)
Ammonia	$NH_4^+ \rightleftharpoons NH_3+H^+$	5.598×10^{-10}	52 220	Alberty and Goldberg (1992)
PCr	$HPCr^{1-} \rightleftharpoons PCr^{2-}+H^+$	8.854×10^{-6}	2660	Alberty and Goldberg (1992)
	$MgPCr \rightleftharpoons PCr^{2-}+Mg^{2+}$	4.305×10^{-3}	–8190	Teague and Dobson (1992), Smith and Alberty (1956)
ATP	$HATP^{3-} \rightleftharpoons ATP^{4-}+H^+$	2.512×10^{-8}	–6300	Alberty and Goldberg (1992)
	$H_2ATP^{2-} \rightleftharpoons HATP^{3-}+H^+$	2.089×10^{-5}	15 000	”
	$MgATP^{2-} \rightleftharpoons ATP^{4-}+Mg^{2+}$	6.607×10^{-7}	–22 900	”
	$Mg_2ATP \rightleftharpoons MgATP^{2-}+Mg^{2+}$	2.042×10^{-3}	–10 800	”
	$HMgATP^{1-} \rightleftharpoons MgATP^{2-}+H^+$	2.344×10^{-4}	–16 900	”
	$KATP^{3-} \rightleftharpoons ATP^{4-}+K^+$	7.488×10^{-3}	0	Smith and Alberty (1956)
ADP	$HADP^{2-} \rightleftharpoons ADP^{3-}+H^+$	6.607×10^{-8}	–5600	Alberty and Goldberg (1992)
	$H_2ADP^{1-} \rightleftharpoons HADP^{2-}+H^+$	4.365×10^{-5}	17600	”
	$MgADP^{1-} \rightleftharpoons ADP^{3-}+Mg^{2+}$	2.239×10^{-5}	–19 000	”
	$HMgADP \rightleftharpoons MgADP^{1-}+H^+$	3.162×10^{-3}	–12 500	”
	$KADP^{2-} \rightleftharpoons ADP^{3-}+K^+$	2.890×10^{-3}	0	Smith and Alberty (1956)
AMP	$HAMP^{1-} \rightleftharpoons AMP^{2-}+H^+$	1.862×10^{-7}	–5400	Alberty and Goldberg (1992)
	$H_2AMP \rightleftharpoons HAMP^{1-}+H^+$	1.023×10^{-4}	18100	”
	$MgAMP \rightleftharpoons AMP^{2-}+Mg^{2+}$	1.622×10^{-3}	–11 300	”
	$KAMP^{1-} \rightleftharpoons ADP^{2-}+K^+$	8.696×10^{-2}	0	Smith and Alberty (1956)
IMP	$HIMP^{1-} \rightleftharpoons IMP^{2-}+H^+$	2.188×10^{-7}	–5983	Phillips *et al.* (1965)
	$H_2IMP \rightleftharpoons HIMP^{1-}+H^+$	1.023×10^{-4}	18100*	
	$MgIMP \rightleftharpoons IMP^{2-}+Mg^{2+}$	7.943×10^{-3}	–11 300*	
	$KIMP^{1-} \rightleftharpoons IMP^{2-}+K^+$	8.696×10^{-2}	0	Smith and Alberty (1956)
Phosphate	$H_2PO_4^{1-} \rightleftharpoons HPO_4^{2-}+H^+$	6.026×10^{-8}	3600	Alberty and Goldberg (1992)
	$MgHPO_4 \rightleftharpoons HPO_4^{2-}+Mg^{2+}$	1.95×10^{-3}	2200	”
	$KHPO_4^{1-} \rightleftharpoons HPO_4^{2-}+K^+$	9.466×10^{-2}	0	Smith and Alberty (1956)

At specified temperature and ionic strength, apparent equilibrium constants (K_{eq}') were calculated using the equation: $\ln K_{eq}' = (-\Delta H°/\boldsymbol{R})(1/T_2-1/T_1)K_{eq}(\Pi\gamma_{substrates}/\Pi\gamma_{products})$, where $\Delta H°$ is the enthalpy (in $J\,mol^{-1}$) of the reaction, $\boldsymbol{R}$ is $8.3145\,J\,K^{-1}\,mol^{-1}$, T_2 is the temperaure in Kelvin, T_1 is the reference temperature of 298.15K, K_{eq} is the reference equilibrium constant at 298.15K and zero ionic strength, $\Pi\gamma_{substrates}$ and $\Pi\gamma_{products}$ are the product of the activity coefficients of substrates and products at specified temperature and ionic strength (Teague and Dobson, 1992). Ion activities were calculated using the extended Debye–Huckel equation: $\ln\gamma = -A_m z_i^2 I^{0.5}/(1+BI^{0.5})$, where A_m is the Debye–Huckel constant described as a function of temperature, z_i is the charge of a species i, B is a constant with a value of $1.61^{1/2}\,mol^{-1/2}$, and I is the ionic strength with a value of 0.25 (see Clarke and Glew, 1980; Goldberg and Tewari, 1991; Tewari and Goldberg, 1991; Alberty and Goldberg, 1992).

*For some of the IMP binding reactions, there was no information available and it was assumed that K_{eq} for IMP was the same as that for AMP (see Curtin and Woledge, 1978). Also, there were very few estimates for K^+ binding, with no description of the effect of temperature.

been examined directly in previous experimental protocols with tuna muscle. Glycogen, lactate and high-energy phosphate levels have been reported for this system (Arthur *et al.* 1992), but estimates of pHi are not available. Model predictions for tuna differ from those of trout primarily because of the increased 'amino buffering' in tuna white muscle (Abe *et al.* 1985; Arthur *et al.* 1993). The results (Fig. 3) predict (1) that while proton load in tuna should exceed that seen in trout muscle, post-exercise pHi should be only marginally lower in the tuna system, (2) that phosphate should bind a substantially smaller proportion of the total proton load than in trout, and (3) that there should be no transient increased acidosis in tuna – the [ADP]/[ATP] ratio should remain approximately constant throughout recovery, such that H^+ concentration should be reflected in changes in the concentration of PCr (see also, Arthur *et al.* 1992, 1993). Future experiments with tuna will look more closely at white muscle acidosis in order test these predicitons. Further adaptions of the model are intended in order to integrate metabolic and acid–base variables that influence pHi in well-perfused oxidative types of muscle.

We thank Dr P. M. Schulte for providing data on muscle pHi. P.W.H. received support from NSERC, and P.G.A. was supported by an MRC postdoctoral fellowship. We thank two anonymous reviewers for very constructive criticisms of early versions of the model.

References

ABE, H., DOBSON, G. P., HOEGER, U. AND PARKHOUSE, W. (1985). Role of histidine-related compounds to intracellular buffering in fish skeletal muscle. *Am. J. Physiol.* **249**, R449–R454.

ALBERTY, R. A. AND GOLDBERG, R. N. (1992). Standard thermodynamic formation properties for the adenosine 5′-triphosphate series. *Biochemistry* **31**, 10610–10615.

ARTHUR, P. G., WEST, T. G., BRILL, R. W., SCHULTE, P. M. AND HOCHACHKA, P. W. (1992). Recovery metabolism of skipjack tuna (*Katsuwonus pelamis*) white muscle: rapid and parallel changes in lactate and phosphocreatine after exercise. *Can. J. Zool.* **70**, 1230–1239.

ARTHUR, P. G., WEST, T. G. AND HOCHACHKA, P. W. (1993). Guides to improving white muscle performance: the roles of glycolysis, phosphogen, lactate and intracellular buffers in tuna. In *Hypoxia and Molecular Medicine*, Proceedings of the 8th International Hypoxia Symposium, Lake Louise, vol. 15, pp. 67–71. Burlington, VT: C. S. Huston Press.

BORCHGREVINK, P. C., BERGAN, A. S., BAKOY, O. E. AND JYNGE, P. (1989). Magnesium and reperfusion of ischemic rat heart as assessed by ^{31}P-NMR. *Am. J. Physiol.* **256**, H195–H204.

BRINLEY, F. J., SCARPA, A. AND TIFERT, T. (1977). The concentration of ionized magnesium in barnacle muscle fibres. *J. Physiol., Lond.* **266**, 545–565.

CLARKE, C. W. AND GLEW, D. N. (1980). Evaluation of Debye–Huckel limiting slopes for water between 0 and 150 °C. *J. chem. Soc. Faraday* **76**, 1911–1916.

CURTIN, N. A. AND WOLEDGE, R. C. (1978). Energy changes and muscular contraction. *Physiol. Rev.* **58**, 690–755.

GOLDBERG, R. N. AND TEWARI, Y. B. (1991). Thermodynamics of the disproportionation of adenosine 5′-diphosphate to adenosine 5′-triphosphate and adenosine 5′-monophosphate. *Biophys. Chem.* **40**, 241–261.

HOCHACHKA, P. W. AND MOMMSEN, T. P. (1983). Protons and anaerobiosis.*Science* **219**, 1391–1397.

JUEL, C. AND WIBRAND, F. (1989). Lactate transport in isolated mouse muscles studied with a tracer technique – kinetics, stereospecificity, pH dependency and maximal capacity. *Acta physiol. scand.* **137**, 33–39.

LINDINGER, M. I. AND HEIGENHAUSER, G. J. F. (1988). Acid–base systems in skeletal muscle and their response to exercise. In *Biochemistry of Exercise*, vol. VII (ed. A. W. Taylor, P. D. Gollnick, H. J. Green, C. D. Ianuzzo, E. G. Noble, G. Metivier and J. R. Sutton), pp. 341–357. Champaign, IL: Human Kinetics Books.

MASON, M. J. AND THOMAS, R. C. (1988). A microelectrode study of the mechanisms of L-lactate entry into and release from frog sartorius muscle. *J. Physiol., Lond.* **400**, 459–479.

MILLIGAN, C. L. AND WOOD, C. M. (1986). Tissue intracellular acid–base status and the fate of lactate after exhaustive exercise in the rainbow trout. *J. exp. Biol.* **123**, 123–144.

MOMMSEN, T. P. AND HOCHACHKA, P. W. (1988). The purine nucleotide cycle as two temporally separated metabolic units: a study on trout muscle. *Metabolism* **37**, 552–556.

MOYES, C. D., SCHULTE, P. M. AND HOCHACHKA, P. W. (1992). Recovery metabolism of trout white muscle: the role of mitochondria. *Am. J. Physiol.* **262**, R295–R304.

MOYES, C. D. AND WEST, T. G. (1995). Exercise metabolism of fish. In *Biochemistry and Molecular Biology of Fishes*, vol. 4, *Metabolic Biochemistry* (ed. P. W. Hochachka and T. P. Mommsen), pp. 367–392. Elsevier: Amsterdam.

MURPHY, E., STEENBERGEN, C., LEVY, L. A., RAJU, B. AND LONDON, R. E. (1989). Cytosolic free magnesium levels in ischemic rat heart. *J. biol. Chem.* **264**, 5622–5627.

PHILLIPS, R., EISENBERG, P., GEORGE, P. AND RUTMAN, R. (1965). Thermodynamic data for the secondary phosphate ionizations of adenosine, guanosine, inosine, cytidine and uridine nucleotides and triphosphate. *J. biol. Chem.* **240**, 4393–4397.

POOLE, R. C. AND HALESTRAP, A. P. (1993). Transport of lactate and other monocarboxylates across plasma membranes. *Am. J. Physiol.* **264**, C761–C782.

PÖRTNER, H.-O. (1987*a*). Contributions of anaerobic metabolism to pH regulation in animal tissues: theory. *J. exp. Biol.* **131**, 69–87.

PÖRTNER, H.-O. (1987*b*). Anaerobic metabolism and changes in acid–base status: quantitative interrelationships and pH regulation in the marine worm *Sipunculus nudus*. *J. exp. Biol.* **131**, 89–105.

PÖRTNER, H.-O. (1990). Determination of intracellular buffer values after metabolic inhibition by fluoride and nitriloacetic acid. *Respir. Physiol.* **81**, 275–288.

PÖRTNER, H.-O., BOUTILIER, R. G., TANG, Y. AND TOEWS, D. P. (1990). Determination of intracellular pH and p_{CO_2} after metabolic inhibition by fluoride and nitrilotriacetic acid. *Respir. Physiol.* **81**, 255–274.

REEVES, R. B. (1972). An imidazole alphastat hypothesis for vertebrate acid–base regulation: tissue carbon dioxide content and body temperature in bullfrogs. *Respir. Physiol.* **14**, 219–236.

SCHULTE, P. M. (1990). Recovery from exhaustive exercise in rainbow trout white muscle: a model for studies of the control of energy metabolism *in vivo*. PhD thesis, University of British Columbia.

SCHULTE, P. M., MOYES, C. D. AND HOCHACHKA, P. W. (1992).

Integrating metabolic pathways in post-exercise recovery of white muscle. *J. exp. Biol.* **166**, 181–195.

SMITH, R. M. AND ALBERTY, R. A. (1956). The apparent stability constants of ionic complexes of various adenosine phosphates with divalent cations. *J. Am. chem. Soc.* **78**, 2376–2380.

STEWART, P. A. (1981). *How to Understand Acid–Base: A Quantitative Acid–Base Primer for Biology and Medicine*. New York: Elsevier-North Holland.

TANG, Y. AND BOUTILIER, R. G. (1991). White muscle intracellular acid–base and lactate status following exhaustive exercise: a comparison between freshwater- and seawater-adapted rainbow trout. *J. exp. Biol.* **156**, 153–171.

TANG, Y., LIN, H. AND RANDALL, D. J. (1992). Compartmental distributions of carbon dioxide and ammonia in rainbow trout at rest and following exercise and the effect of bicarbonate infusion. *J. exp. Biol.* **169**, 235–249.

TANG, Y., MCDONALD, D. G. AND BOUTILIER, R. G. (1989). Acid–base regulation following exhaustive exercise: a comparison between freshwater- and seawater-adapted rainbow trout. *J. exp. Biol.* **141**, 407–418.

TEAGUE, W. E. AND DOBSON, G. P. (1992). Effect of temperature on the creatine kinase equilibrium. *J. biol. Chem.* **267**, 14084–14093.

TEWARI, Y. B. AND GOLDBERG, R. N. (1991). Thermodynamics of the disproportionation of adenosine 5′-triphosphate and adenosine 5′-monophosphate. *Biophys. Chem.* **40**, 263–276.

VAN DEN THILLART, G., VAN WAARDE, A., MULLER, H. J., ERKELENS, C., ADDINK, A. AND LUGTENBURG, J. (1989). Fish muscle energy metabolism measured by *in vivo* ^{31}P-NMR during anoxia and recovery. *Am. J. Physiol.* **256**, R922–R929.

VAN WAARDE, A., VAN DEN THILLART, G., ERKELENS, C., ADDINK, A. AND LUGTENBURG, J. (1990). Functional coupling of glycolysis and phosphocreatine utilization in anoxic fish muscle – an *in vivo* P-31 NMR study. *J. biol. Chem.* **265**, 914–923.

WESTERBLAD, H., LEE, J. A., LANNERGREN, J. AND ALLEN, D. G. (1991). Cellular mechanisms of fatigue in skeletal muscle. *Am. J. Physiol.* **261**, C195–C209.

WOOD, C. M. (1991). Acid–base and ion balance, metabolism and their interactions, after exhaustive exercise in fish. *J. exp. Biol.* **160**, 285–308.